Journal of Hydrology: Regional Studies 14 (2017) 37–48

Contents lists available at ScienceDirect

Journal of Hydrology: Regional Studies

journal homepage: www.elsevier.com/locate/ejrh

Stable isotopes of river water and groundwater along altitudinal gradients in the High Himalayas and the Eastern Nyainqentanghla Mountains

Lee Florea[a,*], Broxton Bird[b], Jamie K. Lau[e], Lixin Wang[b], Yanbin Lei[c], Tandong Yao[c], Lonnie G. Thompson[d]

[a] Indiana Geological and Water Survey, Indiana University, 611 Walnut Grove, Bloomington, IN, 47405, United States
[b] Department of Earth Sciences, Indiana University-Purdue University Indianapolis, IN, United States
[c] Institute of Tibetan Plateau Research – Chinese Academy of Sciences, Beijing, China
[d] The Byrd Polar and Climate Research Center, The Ohio State University, Columbus, OH, United States
[e] Department of Biology, Radford University, Radford VA 24142, United States

ARTICLE INFO

Keywords:
Nepal
China
Tibetan plateau
Deuterium excess
Local water line

ABSTRACT

Study Region This study considers river water and groundwater in seeps and springs collected from the non-monsoon season in the valleys of the Dudh Koshi River in eastern Nepal and the Niyang River of eastern Tibet, both in the Himalaya Mountains.

Study Focus Data from this study comprise water samples that provide a single season snapshot of $\delta^{18}O$ and δD values that give additional information into the sources of moisture and the altitude lapse rates for the southern flank of the High Himalaya of Nepal and the Eastern Nyainqentanghla Mountains of the Tibetan Plateau.

New Hydrological Insights The local water line for Nepal samples, $\delta D = (7.8 \pm 0.3) \cdot \delta^{18}O + (4.0‰ \pm 4.6‰)$, was moderately lower in slope than for Tibetan Plateau samples, $\delta D = (8.7 \pm 0.1) \cdot \delta^{18}O + (24.3‰ \pm 2.0‰)$; evaporation has a greater influence on the Nepal samples—consistent with warmer temperatures in Nepal versus Tibet within the same altitude range. Mean d-excess values for Tibet samples (13.1‰ ± 2.0‰) implies that recycled continental moisture has more influence than marine moisture observed for the Nepal samples (7.4‰ ± 4.4‰). Altitude lapse rates of $\delta^{18}O$ and δD for Nepal samples (-2.8‰‰ km^{-1} and $-24.0‰\ km^{-1}$) do not significantly differ from Tibet samples ($-3.1‰‰\ km^{-1}$ and $-27.0‰\ km^{-1}$) and regional measurements; the lapse rates are reduced above 4500 m and are not influenced by exceptionally high elevations in the Dudh Koshi River watershed.

1. Introduction

Stable isotopes of hydrogen and oxygen are one method used to model hydrological cycles and determine sources of water (Dansgaard, 1964; Gat, 1996; Bowen and Wilkinson, 2002). The isotopic composition is commonly reported in the standard delta notation.

$$\delta = (R_{sample}/R_{standard} - 1) \cdot 1000‰, \quad (1)$$

* Corresponding author.
E-mail address: lflorea@indiana.edu (L. Florea).

http://dx.doi.org/10.1016/j.ejrh.2017.10.003
Received 24 March 2017; Received in revised form 25 September 2017; Accepted 18 October 2017
Available online 05 November 2017

where R is the ratio of heavy to light isotope. differences in climate leads to differences in δ^2H and $\delta^{18}O$ between geographically separated reservoirs of surface water and groundwater. These isotopes are heavily influenced by regional climate and are used to estimate effects of evaporation on a water body (Dailai et al., 2002; Jeelani et al., 2013) and as an altimeter for orographic uplift—an 'altitude effect' (Clark and Fritz, 1997). The linear relationship between δ^2H and $\delta^{18}O$ is one means to assess the cumulative effects of fractionation caused by evaporation and condensation in samples of precipitation (local meteoric water line, LMWL) and surface/shallow groundwaters (local water line, LWL) as compared to the global equilibrium between evaporation and condensation (global meteoric water line, GMWL) defined by the relation:

$$\delta D = 8 \cdot (\delta^{18}O) + 10‰ \quad (2)$$

(Craig, 1961; Ambach, 1968). LWLs may deviate from the GMWL during any non-equilibrium event, such as evaporation, mixing, or additional input of marine moisture. For example, LWLs with slopes less than or greater than 8 can indicate systems dominated by evaporation and recharge/recycled moisture, respectively (Craig, 1961).

During evaporation, δD of the produced moisture decreases less rapidly than $\delta^{18}O$ compared to the slope of 8 of the GMWL, leading to samples that lie above the GMWL. In contrast, remaining water in the evaporated source will have values below the GMWL leading to LWL with slopes less than 8. The deuterium excess (Dansgaard, 1964), calculated for each sample as

$$\text{d-excess} = \delta D - 8 \cdot (\delta^{18}O), \quad (3)$$

can reveal changes in sources of moisture for precipitation. Values of d-excess greater than 10‰ may indicate recycling of water sources, snow formation, and cooler/dry air masses. In contrast, d-excess values less than 10‰ may indicate secondary evaporation (e.g. from cloud formation or terrestrial waters) and more humid air masses. For example, d-excess in the Tibetan Plateau of China changes per the monsoon (Liu et al., 2008); lower d-excess values from north-migrating moisture from the Indian Ocean during the summer and higher d-excess values derived from drier continental air during the winter months—a 'continental effect' (Clark and Fritz, 1997) produced by multiple cycles of evaporation and precipitation (Gat and Matsui, 1991).

The altitude affect has been studied in Himalayas precipitation and surface waters (Dailai et al., 2002; Wen et al., 2012; Jeelani et al., 2013). Isotopically heavier water falls first during a precipitation event; thus, $\delta^{18}O$ and δD values decrease during progressive precipitation from adiabatic cooling along an altitude gradient—an altitude lapse rate (Dansgaard, 1964; Clark and Fritz, 1997). The altitude lapse rate for precipitation in the Kashmir Himalayas measured $-2.3‰\ km^{-1}$ for $\delta^{18}O$ and $-12‰\ km^{-1}$ for δD (Jeelani et al., 2013). In the southern Himalayass, the altitude lapse rate for $\delta^{18}O$ was lower during the monsoon season (-1.5‰ km^{-1}) compared to the non-monsoon season ($-2.3‰\ km^{-1}$) (Wen et al., 2012). In the Yamuna River in the northwestern Himalayas, the altitude lapse rate for the non-monsoon season was $-1.1‰\ km^{-1}$ for $\delta^{18}O$ and $-12‰\ km^{-1}$ for δD (Dailai et al., 2002). In the Boqu River in the southern Himalayas, the altitude lapse rate during the monsoon season was $-3.6‰{\cdot}km^{-1}$ for $\delta^{18}O$ (Wen et al., 2012).

Similarly, LWLs and d-excess have been studied in Himalayas precipitation and surface waters (Pande et al., 2000; Dailai et al., 2002). Rivers sampled spanning the Himalayas have produced LWLs with a slope greater than the GMWL and with d-excess values greater than 10‰ (Pande et al., 2000). Combing precipitation data, Pande et al. (2000) concluded that snowfall contributed to greater slopes and that contributing moisture derived in part from Mediterranean air masses. In the Yamuna River in the northwestern Himalayas, tributaries sampled during the monsoon season were depleted in ^{18}O and ^{2}H (Dailai et al., 2002)—a product of the 'amount effect' where increased precipitation leads to lower values of $\delta^{18}O$ and δD (Dansgaard, 1964). Further, Dailai et al. (2002) compared LWLs produced from samples collected during the monsoon and non-monsoon season and found that the LWL of the monsoon season correlated well with the predicted effects of the monsoon rains, i.e. the LWL fell above the GMWL. Similarly, the LWL of the non-monsoon season fell below the GMWL, indicating that the river was dominated by evaporation. Values of d-excess from precipitation of the Kashmir Himalayas were low during the monsoon (3.2–12.8‰) from evaporating rainfall derived from moisture sources in the Indian Ocean, and high during the non-monsoon season (20–22‰) from recycled moisture derived from the Mediterranean (Jeelani et al., 2013)

In this study, we present a single-season snapshot of the isotopic composition of river water and groundwater sampled in the Dudh Koshi River watershed in the Himalayas of eastern Nepal and in the Niyang River watershed in the Eastern Nyainqentanghla Mountains of Tibet, China. The isotopic compositions of river water and groundwater in the Dudh Koshi and Niyang River sites have not been evaluated prior to this study, and present an interesting comparison between a tributary of the Ganges River on the south flank of the Himalayas Range in Sagarmantha National Park (Dudh Koshi River) and a tributary of the Brahmaputra River north of the Himalayas crest on the Tibetan Plateau (Niyang River); both are headwater streams that drain to the Indian Ocean.

The present study compares the altitude lapse rates, assess the role of evaporation between these locations, and provide one benchmark for future studies of the hydrological cycle in these portions of the Himalaya Mountains. Aside from questions of strict comparisons between data explored in this manuscript, one motivating purpose is better understand residence times of shallow groundwater to assist with the management of sustainable water supplies in communities with significant tourism demand (Manfredi et al., 2010). Another interesting question is whether the presence of seven mountain peaks exceeding 8,000 ma.s.l. in the region surrounding the Dudh Koshi watershed results in an altitude lapse rate sizably different that elsewhere in the Himalayas Mountains.

2. Physical setting

The Dudh Koshi River watershed in the southern Himalaya spans 3712 km^2 and is located just south of Mount Everest in Nepal, a significant portion within the boundaries of Saragmantha National Park, and includes the towns of Lukla and Namche Bazar (Fig. 1).

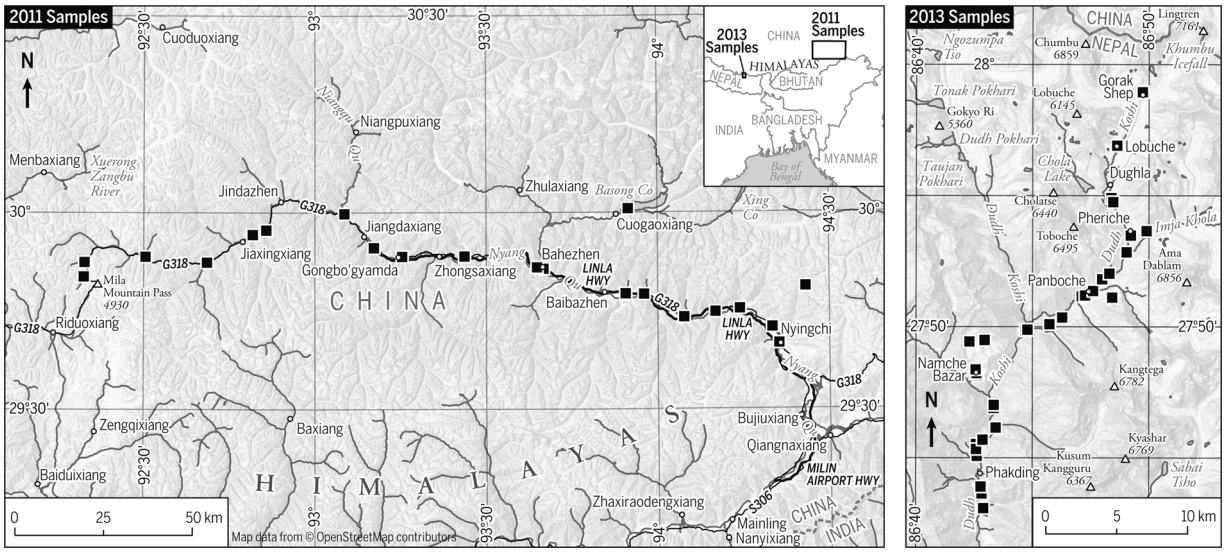

Fig. 1. Sampling locations in the Dudh Koshi River watershed in the High Himalayas of Nepal (2013 samples − right) and the Niyang River watershed in the Eastern Nyainqentanghla, China (2011 samples − left).

Headwaters emerge largely from glaciers at elevations greater than 4800 m above sea level (m.a.s.l.), including the Khumbu Glacier on the southwest flank of Everest. These glaciers originate at elevations above 7,500 ma s l. The Niyang River watershed in the Eastern Nyainqentanghla Mountains covers 24,800 km^2 east of Lhasa, China (Fig. 1); headwaters originate on the Tibetan Plateau at elevations less than 5,500 ma s l. and from minimal glacial ice.

The physiography of the southern and northeastern Himalaya differs. Both are mountainous landscapes; however, the Dudh Koshi River originates from the crest of the Himalaya uplift and flows south toward the Ganges lowlands while the Niyang River flows east through the Nyainqentanghla Mountains before joining the Yarlung Tsangpo/Brahmaputra River. Terrestrial ecoregions in these two locations were identified using global data described by Olson et al. (2001). Sites above 3,600 ma s l. in altitude in the southern Himalayas are dominated by alpine shrub and meadows; sites below 3,600 ma s l. in altitude are dominated by subalpine conifer forests (Olson et al., 2001). Sites above 4,600 ma s l. in altitude in the Nyainqentanghla Mountains are dominated by shrublands and meadows; sites below 4,600 ma s .l. in altitude are dominated by subalpine conifer forests (Olson et al., 2001).

The hydrology of the two study locations differs. Average stream gradients, calculated using GIS, are much greater in the Dudh Koshi River (71 m km^{-1}) than for the Niyang River (8 m km^{-1}). Regionally, more than 85% of the annual precipitation occurs from May to September, during the summer monsoon season (Garzione et al., 2000). According to the Köppen-Geiger climate classification, locations in the Dudh Koshi River watershed above 3,600 ma s l. are dominated by a polar tundra climate (IVPA, 2011) with temperatures between 0 °C and 10 °C in the summer (Peel et al., 2007). Similarly, locations in the Niyang River watershed above 4,600 ma s l. are dominated by a polar tundra climate (the elevation of this boundary decreases to 4,200 ma s l. in the headwaters). Lower elevations in both watersheds are characterized by a transition from dry, snowy winters and cool summers (less than 4 months with temperatures > 10 °C) to dry winters and warm wet summers. This transition in the Niyang River watershed, which has a lower stream gradient, occurs over a greater distance (Peel et al., 2007).

Daily climate measures were averaged over sampling time frames using historical data from the several Meteorological Assimilation Data Ingest System (MADIS), private, and airport weather stations (Weather Underground, 2014). Average daily temperatures were warmer in the High Himalayas in March 2013 (17.9 °C) compared to the Nyainqentanghla Mountains in May 2011 (14.0 °C). Total precipitation for these same time ranges was lower in the High Himalayas (2.0 mm) compared to the Nyainqentanghla Mountains (9.4 mm). The average percent humidity was higher in the High Himalayas (56%) compared to Nyainqentanghla Mountains (45%). Both sets of samples were collected during the non-monsoon season (Wen et al., 2012) and values of the Oceanic Niño Index (ONI) archived by the National Oceanic and Atmospheric Administration (NOAA, 2017) are similar for both sampling periods (-0.4 for March 2013 and −0.2 for May 2011) however, stronger La Niña conditions were present leading up to the 2011 sample collection in the Tibetan Plateau. In contrast, data presented by Wen et al. (2012) spans the years 1997–2010 and includes multiple oscillations of the ONI index.

3. Methods

Water samples were collected during the non-monsoon season at increasing altitudes in the Dudh Koshi watershed in the southern Himalayas of Nepal (n = 32; 2013/3/3–2013/3/13) and in the Niyang watershed of the northeastern Himalayas in Tibet (n = 22; 2011/5/15–2011/5/20) (Fig. 1). Of the 32 samples collected in Nepal, 22 were from groundwater seeps and springs, 5 were from tributary streams, and 5 were from the main channel along a 40 km-long segment of the Dudh Koshi River (Table 1). Of the 22 samples collected from Tibet, 14 were from tributary streams and 8 were from the main channel along a 255 km-long segment of the

Table 1
The mean δ18O, δD, and d-excess values reported as per mil for sites sampled in the southern Himalayans, Nepal, March 2013.

Site no.	Name	Altitude (m)	$\delta^{18}O$	δD	d-excess
O3A	Thrdokoshi River	2550	−12.8	−89.5	12.5
O3B	Small spring pipe	2621	−11.0	−83.1	5.2
O3C	Small spring pipe	2576	−9.7	−67.8	9.7
O4A	Ghatte Kola Major Trib	2701	−8.8	−64.7	5.7
O4B	Toc-Toc Falls	2746	−9.7	−73.4	4.4
O4C	Small waterfall	2782	−10.4	−73.0	10.2
O4D	Hillside flow	2734	−10.1	−75.4	5.4
O4E	Monju River	2804	−14.7	−107.8	9.8
O4F	Dudhkoshi River	2825	−14.8	−106.4	12.2
O4G	East tributary north of Monju	2839	−11.0	−75.2	12.7
O4H	Namche Bazar south water supply	3411	−12.7	−88.0	13.4
O5A	Namche Bazar water supply	3417	−13.2	−95.8	9.7
O5B	Spring above Namche Bazar	3508	−12.4	−91.9	7.1
O6A	Khumjung water supply	3800	−11.0	−84.3	4.0
O6B	Khunde water supply	3874	−13.2	−97.7	7.6
O7A	Hose from hillside	3307	−12.6	−98.2	2.3
O7B	Phorte Thenga water supply	3315	−13.9	−100.0	11.0
O7C	Spring below Tengboche	3810	−12.6	−91.3	9.9
O8A	Deboche spring	3746	−10.6	−85.9	−1.2
O8B	Hillside seep	3895	−14.0	−103.6	8.0
O8C	Spring south of Pangboche	3895	−14.6	−107.9	8.9
O8D	Stream north of Pangboche	3947	−14.2	−104.0	9.3
O8E	Seep west side	3834	−12.9	−102.7	0.4
O8F	Shomore water supply	4009	−15.1	−109.5	11.4
O8G	Khumba River	4168	−15.2	−116.0	5.4
O8H	Dingboche spring	4351	−15.3	−120.5	1.7
10A	Khumba outflow	4604	−17.9	−129.3	13.8
10B	Labuche water supply	4929	−15.7	−118.9	6.9
11A	Gorak shep water supply	5180	−15.9	−132.1	−4.8
12A	Sping at base of Dinbuche Ridge	4376	−16.3	−122.8	7.5
12B	Sping at base of Dinbuche Ridge	4399	−15.9	−120.4	7.0
12C	Perrochet water supply	4292	−15.7	−115.6	10.1
			−13.2	−98.51	7.40438
			2.3	18.332	4.37677

Niyang River (Table 2). Sampling procedures were dictated by site conditions: groundwaters from seeps, springs, and domestic water supplies were collected either at the source or at the outflow of the delivery pipe; river waters were collected along the stream bank using a syringe to gather the sample > 10 cm below the surface and transfer to small (< 15 mL) borosilicate vials. In all instances, the samples represent a representative sample collected from a thoroughly mixed site. Sample sites with significant suspended sediments were filtered. Once back in the lab, the samples were stored at 4 °C until analysis.

Table 2
Summary comparing the altitude effect among water sources and the local water lines between the High Himalayas and the Tibetan Plateau.

Altitude Effect	*df* (min, total)	*F*	*p*
Dudh Koshi vs. Niyang			
$\delta^{18}O$	1, 50	0.63	0.43
δD	1, 50	1.07	0.31
d-excess	1, 50	0.024	0.63
Dudh Koshi sample types			
$\delta^{18}O$	1, 50	0.063	0.43
δD	1, 50	1.07	0.31
d-excess	1, 50	0.24	0.63
Niyang sample types			
$\delta^{18}O$	1, 20	4.72	0.04
δD	1, 21	4.78	0.04
d-excess	1, 22	0.55	0.22
Local Water Lines	1, 50	3.99	0.05

df = ° of freedom, F = F-statistic in least squares ANOVA, p = p-value in least squares ANOVA.

3.1. Measurement of $\delta^{18}O$ and δD

The water samples from Nepal were measured with a LGR Triple Water Vapor Isotope Analyzer (T-WVIA), Model 45-EP. The measurements had an analytical precision of ± 0.2‰ for $\delta^{18}O$ and ± 0.8‰ for δD (Wang et al., 2009). The T-WVIA results were reported in per mil (‰) and corrected using standards referenced to Vienna Standard Mean Ocean Water (V-SMOW), which was analyzed prior each batch of water samples. Briefly, samples and standards were injected into the LGR vaporizer by inserting a capillary tube into the vial. Measurements each second were collected for a duration of one minute for samples and two minutes for standards. The T-WVIA was flushed before and after each sample to avoid transient effects from switching the capillary tube from vial to vial (Wang et al., 2010). During each flush, vapor concentrations were allowed to reach ambient levels (< 200 ppm).

Water samples from Tibet were analyzed for $\delta^{18}O$ and δD using a Picarro L2130-i Analyzer coupled to an auto sampler and high-precision water vaporizer unit. Measurements were corrected for memory and drift following the methodology of Geldern and Barth (2012). Final values were corrected to the VSMOW scale using calibrated standards from Los Gatos. Precision for $\delta^{18}O$ and δD is 0.1‰ and 0.6‰, respectively.

3.2. Statistical treatment

Linear regressions were used to determine whether a significant altitude effect in values of $\delta^{18}O$, δD, and d-excess exists in the southern and northeastern Himalayas. Altitude was the predictor variable while $\delta^{18}O$, δD, and d-excess were each the response variables. Further, a general linear model was used to determine whether the altitude effect was significantly different between the southern and northeastern Himalayas.

A linear regression analysis was used to evaluate the relationship between δD and $\delta^{18}O$, d-excess, and LWLs. Similarly, a general linear model using a least squares regression ANOVA was used to determine whether populations were significantly different between water types and between the southern and northeastern Himalayas. All statistical treatments were considered significant at $p = 0.05$.

4. Results

4.1. Isotopic values and local water lines

In the Dudh Koshi River watershed, $\delta^{18}O$ values ranged from −9.7‰ to −17.9‰, while the values of δD ranged from −73.0‰ to −132.1‰. The LWL for these samples was $\delta D = (7.8 \pm 0.3) \cdot \delta^{18}O + (4.0‰ \pm 4.6‰)$ ($r^2 = 0.94$, $p < 0.001$; Fig. 2). Even though samples from tributary streams originated from sources at lower elevations relative to the glacial outlet of the Dudh Koshi River, and thus show as independent populations on the LWL, individual sample types produced LWLs of similar slope. More specifically, the $\delta^{18}O$ values for groundwater ranged from −9.7‰ to −16.3‰, while the values of δD ranged from −67.8‰ to −132.1‰. $\delta^{18}O$ values for river tributaries ranged from −8.8‰ to −14.2‰, while the values of δD ranged from −64.7‰ to −104.

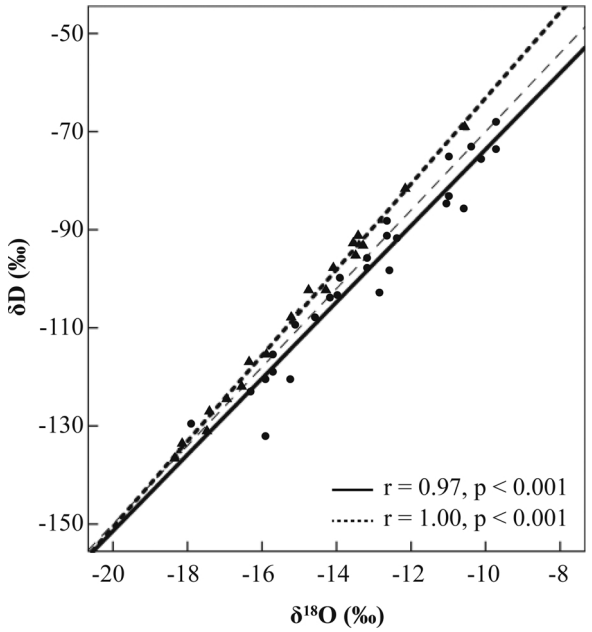

Fig. 2. The local water line for samples from the Dudh Koshi watershed in the Southern Himalayas of Nepal (solid circles and solid line), and for samples from the Niyang watershed of the Tibetan Plateau in China (solid triangles and thick dotted line). The global meteoric water line (GMWL) is represented by the thin dashed line. All values are referenced to V-SMOW. Analytical precision is within the scale of the symbol.

Table 3
The mean δ18δ18O, δD, and d-excess values reported as per mil for sites sampled in the northeastern Himalayans, China, May 2011.

Site no.	Name	Altitude (m)	$\delta^{18}O$	δD	d-excess
7	Niyang River at site 7	4780	−18.3	−136.4	10.0
9	Niyang River 1	3000	−13.3	−92.9	13.4
10	Cuomujiri	4085	−13.5	−95.4	12.7
11	Niyang River 2	3010	−14.3	−102.4	12.1
12	Niyang River tributary 1	3070	−12.1	−81.5	15.6
13	Niyang River tributary 2	3080	−10.5	−69.3	15.0
14	Niyang River tributary 3	3100	−12.8	−88.2	14.4
15	Niyang River tributary 4	3140	−14.1	−97.9	15.0
16	Niyang River tributary 5	3150	−13.4	−92.8	14.4
17	Niyang River tributary 6	3220	−15.0	−106.6	13.5
18	Niyang River 3	3230	−15.2	−107.7	13.9
19	Niyang River tributary 7	3335	−13.4	−91.4	16.1
20	Niyang River tributary 8	3430	−13.5	−92.6	15.4
21	Niyang River tributary 9	3470	−14.8	−102.4	15.6
22	Niyang River 4	3540	−16.6	−121.9	10.6
23	Niyang River tributary 10	3780	−16.3	−116.9	13.7
24	Niyang River tributary 11	3800	−15.9	−115.4	11.7
25	Niyang River tributary 12 (SW)	3990	−17.0	−124.4	11.5
26	Niyang River tributary 13 (W #6)	3990	−17.4	−127.2	12.0
27	Niyang River 6	4250	−17.5	−130.9	9.0
28	Niyang River tributary 14	4630	−18.1	−133.5	11.6
29	Niyang River 7	4780	−18.2	−135.2	10.7
			−15.1	−107.4	13.0809
			2.1665	18.9823	2.039808

0‰. $\delta^{18}O$ values for river main channels ranged from −12.8‰ to −17.9‰, while the values of δD ranged from −89.5‰ to −129.3‰ (Table 1).

Deuterium excess of groundwater in the Dudh Koshi watershed ranged between −4.8‰ to 13.4‰. Tributary streams and the Dudh Koshi River had overlapping d-excess with groundwater, with values ranging between 4.4‰ to 12.7‰ and 5.4‰ to 13.8‰, respectively. The three sample types were not significantly different ($p > 0.05$; Table 2).

In the Niyang River watershed, $\delta^{18}O$ values ranged from −10.5‰ to −18.3‰, while the values of δD ranged from −69.3‰ to −136.4‰. The LWL for these samples was $\delta D = (8.7 \pm 0.1) \cdot \delta^{18}O + (24.3‰ \pm 2.0‰)$ ($r^2 = 1.00$, $p < 0.001$; Fig. 2). $\delta^{18}O$ values for tributaries streams ranged from −10.5‰ to −18.1‰, while the values of δD ranged from −69.3‰ to −133.5‰. $\delta^{18}O$ values for river main channels ranged from −13.3‰ to −18.3‰, while the values of δD ranged from −92.9‰ to −136.4‰ (Table 3). Like the Nepal samples, individual sample types produced LWLs of similar slope. However, the LWLs between the Dudh Koshi River and Niyang River watersheds are significantly different ($p = 0.05$; Table 2).

d-excess values were significantly higher on the Tibetan Plateau than in Nepal ($df = 37.7$; $t = 6.1$, $p < 0.001$) and ranged from 9.0‰ to 16.1‰ (Table 3). For tributary streams of the Niyang, the range in d-excess values was 11.5‰ to 16.1‰. Samples from the Niyang River had somewhat lower d-excess values ranging between 9.0‰ and 13.9‰. Samples from the Niyang watershed are more tightly clustered, and the populations of samples from tributary streams and the river were not significantly different ($p > 0.05$; Table 2).

4.2. Altitude lapse rates

The altitude lapse rate for samples in the Dudh Koshi River watershed measured $-2.8‰\ km^{-1}$ for $\delta^{18}O$ ($r^2 = 0.76$, $p < 0.001$; Fig. 3A) and $-24.0‰\ km^{-1}$ for δD ($r^2 = 0.85$, $p < 0.001$; Fig. 3B). The intercept for $\delta^{18}O$ was −2.8‰ and for δD −9.8‰. More specifically, the altitude lapse rate for groundwater samples was $-2.5‰{\cdot}km^{-1}$ for $\delta^{18}O$ ($r^2 = 0.69$, $p < 0.001$; Fig. 4A) and $-22.3‰\ km^{-1}$ for δD ($r^2 = 0.80$, $p < 0.001$; Fig. 4B) with intercepts of −3.8‰ for $\delta^{18}O$ and −16.2‰ for δD. The altitude lapse rate for river tributaries was $-3.7‰\ km^{-1}$ for $\delta^{18}O$ ($r^2 = 0.90$, $p < 0.05$; Fig. 4A) and $-27.9‰{\cdot}km^{-1}$ for δD ($r^2 = 0.96$, $p < 0.05$; Fig. 4B) with intercepts of −0.2‰ for $\delta^{18}O$ and −5.7‰ for δD. The altitude lapse rate for samples from the Dudh Koshi River was $-1.7‰\ km^{-1}$ for $\delta^{18}O$ ($r^2 = 0.73$, $p = 0.07$; Fig. 4A) and $-14.1‰\ km^{-1}$ for δD ($r^2 = 0.81$, $p < 0.05$; Fig. 4B) with intercepts of −9.4‰ for $\delta^{18}O$ and −61.9‰ for δD. The altitude lapse rates among the three sample types were not significantly different ($p > 0.05$; Table 2).

The altitude lapse rate for samples in the Niyang River watershed measured $-3.1‰\ km^{-1}$ for $\delta^{18}O$ ($r^2 = 0.68$, $p < 0.001$; Fig. 3A) and $-24.0‰\ km^{-1}$ for δD ($r^2 = 0.69$, $p < 0.001$; Fig. 3B). The intercept for $\delta^{18}O$ was −4.0‰ and for δD −9.7‰. More specifically, the altitude lapse rate for river tributaries was $-4.1‰\ km^{-1}$ for $\delta^{18}O$ ($r^2 = 0.79$, $p < 0.001$; Fig. 5A) and $-35.9‰\ km^{-1}$ for δD ($r^2 = 0.80$, $p < 0.001$; Fig. 5B) with intercepts of −0.06‰ for $\delta^{18}O$ and 23.3‰ for δD. The altitude lapse rate for samples from the Niyang River was $-2.1‰\ km^{-1}$ for $\delta^{18}O$ ($r^2 = 0.60$, $p < 0.05$; Fig. 5A) and $-18.6‰{\cdot}km^{-1}$ for δD ($r^2 = 0.60$, $p < 0.05$; Fig. 5B) with intercepts of −7.7‰ for $\delta^{18}O$ and −43.4‰ for δD. The altitude lapse rates among the two sample types were significantly different ($p < 0.05$; Table 2); however, the lapse rate values are not significantly different between the two watersheds ($p > 0.05$; Table 2).

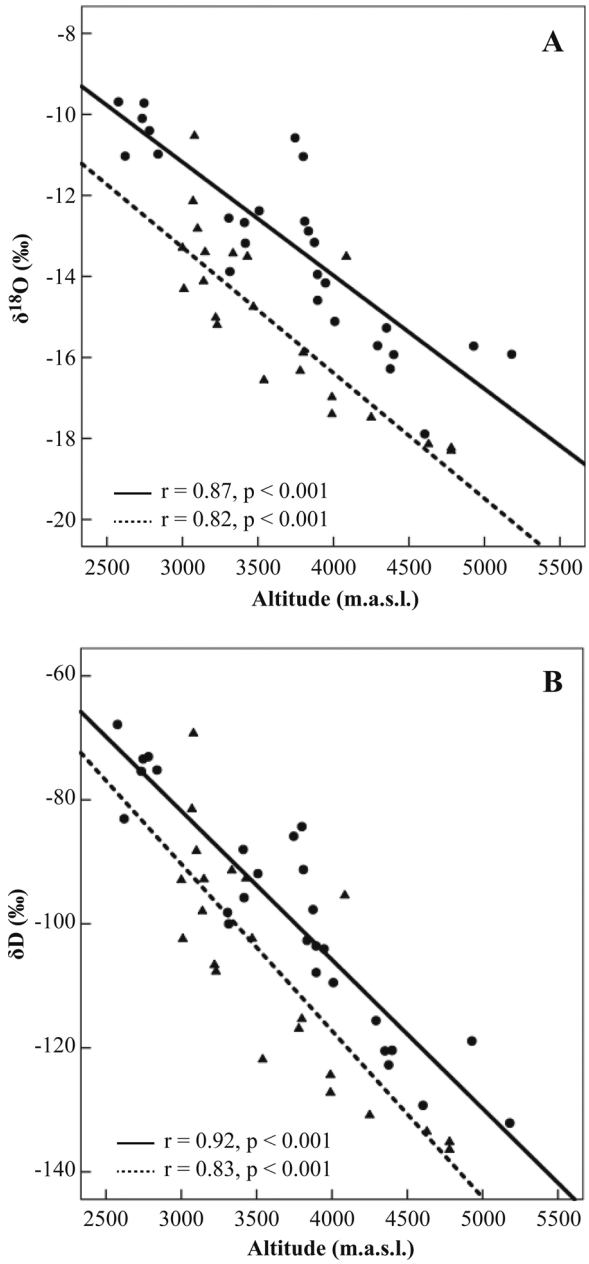

Fig. 3. Relationship between altitude and $\delta^{18}O$ (A) and $\delta^{2}H$ (B) for samples from the Dudh Koshi watershed in the Southern Himalayas of Nepal (solid circles and solid line), and for samples from the Niyang watershed of the Tibetan Plateau in China (solid triangles and thick dotted line). All values are referenced to V-SMOW. Analytical precision is within the scale of the symbol.

5. Discussion

Data presented in this study provide one glimpse into the spatial variability of $\delta^{18}O$ and δD in the Himalayas Mountains. The location of samples complement published datasets for precipitation and surface waters elsewhere in the southern Himalayas (Garzione et al., 2000; Wen et al., 2012), the western Himalayas (Jeelani et al., 2013; Dailai et al., 2002), the Tibetan Plateau (Tian et al., 2001; Hren et al., 2009), and the Ganges Lowlands (Pang et al., 2004). The measurements can increase the sensitivity of regional isoscape models, such as that presented by Bershaw et al. (2012) for the Himalayas and Tibetan Plateau. They are the first that look at the isotopic composition of shallow groundwater of the High Himalaya. They also are the first published for sites in Sagarmantha National Park along the trail to Everest Basecamp, a region increasingly strapped for water resources.

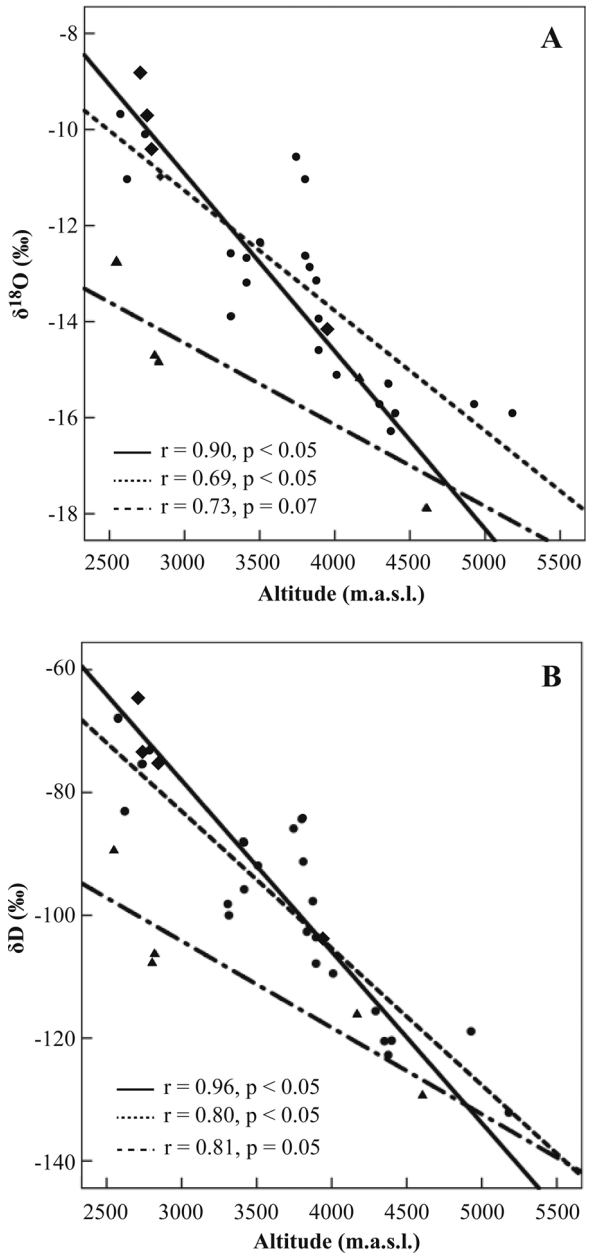

Fig. 4. Relationship between altitude and $\delta^{18}O$ (A) and $\delta^{2}H$ (B) in ground water (solid circles and dashed line), tributary streams (solid diamonds and solid line), and the Dudh Koshi River (solid triangles and dash-dot line) for samples from the Dudh Koshi watershed in the southern Himalayas of Nepal. All values are referenced to V-SMOW. Analytical precision is within the scale of the symbol.

5.1. Local water lines (LWL)

Surface waters and shallow groundwater isotopes are homogenized from regional trends in precipitation, modified by evaporation, and are thus greatly influenced by latitude, elevation, and patterns of climate. In the case of the samples from the Dudh Koshi River watershed, the slope of the LWL (7.8) and the range of d-excess values (< 10‰) are suggestive of monsoonal sources of Indian Ocean precipitation that has experience significant evaporation during the non-monsoon season. The LWL result resembles that published for surface waters in the Kali Gandaki watershed west of Mount Everest and Katmandu ($\delta D = 7.6 \cdot \delta^{18}O + 5.7‰$; Garzione et al., 2000), precipitation in the Kashmir Himalaya of northwest India ($\delta D = 7.6 \cdot \delta^{18}O + 11.8‰$; Jeelani et al., 2013), and for rainfall in New Delhi, India ($\delta D = 7.1 \cdot \delta^{18}O + 3.5‰$; Pang et al., 2004). Similar LMWL results have also been identified for precipitation on the Qilian Mountains on northeast slope of the Tibetan Plateau (Feng et al., 2017); however, the relatively high average d-excess values in that study are consistent with stronger influence by continental sources of moisture.

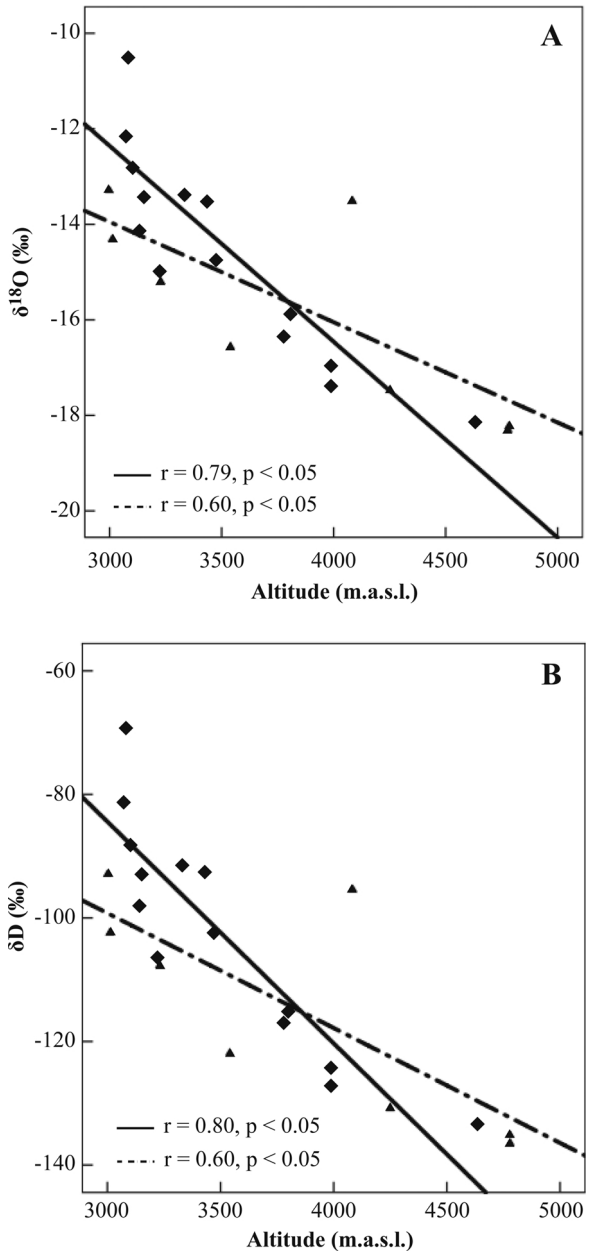

Fig. 5. Relationship between altitude and $\delta^{18}O$ (A) and $\delta^{2}H$ (B) in tributary streams (solid diamonds and solid line) and the Niyang River (solid triangles and dash-dot line) for samples from the Niyang watershed in the northeast Himalayas of Tibet. All values are referenced to V-SMOW. Analytical precision is within the scale of the symbol.

For the Niyang River watershed, the slope of the LWL (8.7) and the range of d-excess values (> 10‰), indicate a system recharged by sources of recycled moisture derived from continental sources in addition to monsoonal moisture (Yao et al., 2009). In both watersheds, the d-excess values tend to decrease with altitude (Fig. 6), though only the trend for the Niyang River is significant ($p < 0.05$). Fan et al. (2014), using data from northwest China did not find a correlation between d-excess and elevation; interestingly, however, that study did find a correlation between d-excess and surface air temperature for the same data. The increasing d-excess along the river length, particularly in the Niyang River watershed, are an indication of evaporation rates and air temperatures both increasing at lower elevation. Glacial melt is the most significant water source for river water in the Dudh Koshi River watershed thus, d-excess values for those river samples demonstrate no trend with altitude (Table 1).

The differences between the Dudh Koshi River and Niyang River data are prominent despite similar latitude (30°N in Tibet versus 28°N in Nepal) and elevation ranges (3000-4,780 ma.s.l. in Tibet versus 2550-5,180 ma.s.l. in Nepal), suggesting the significant influence of a Himalaya rain shadow. Samples values from the Dudh Koshi watershed ($\delta^{18}O = -13.2‰ \pm 2.3‰$; $\delta D = -98.5‰ \pm 18.3‰$) are on the windward side of the Himalayas front during monsoonal transport of marine moisture and are

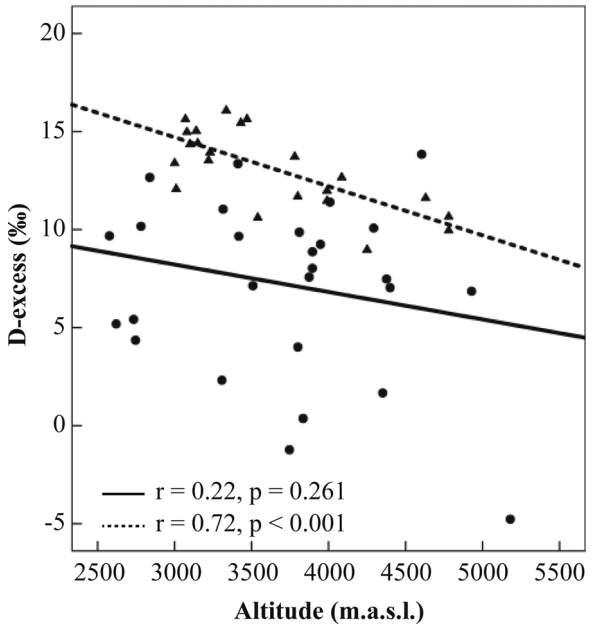

Fig. 6. Relationship between altitude and d-excess in the Dudh Koshi watershed in the Southern Himalayas of Nepal (solid circles and solid line), and for samples from the Niyang watershed of the Tibetan Plateau in China (solid triangles and thick dotted line). All values are referenced to V-SMOW. Analytical precision is within the scale of the symbol.

less isotopically depleted by the amount effect during orographic uplift (Clark and Fritz, 1997) than the samples from the Niyang River watershed ($\delta^{18}O = -15.1‰ \pm 2.2‰$; $\delta D = -107.4‰ \pm 19.0‰$).

The LWL for the Niyang River watershed is like others published for the Tibetan Plateau. For example, Tian et al. (2001) compiled six LMWLs across the plateau and a LWL for several rivers; all but one of those returned slopes > 8 and d-excess values > 10‰ (the exception being precipitation in Lhasa in the southern plateau). Hren et al. (2009) and Pande et al. (2000) also found similar relationships for rivers in the Tibetan Plateau ($\delta D = 8.2 \cdot \delta^{18}O + 17.5‰$ and $\delta D = 8.7 \cdot \delta^{18}O + 29.9‰$).

Significant scatter exists in the Nepal data, both in terms of the LWLs and d-excess (Figs. 2 and 6). This scatter includes samples from river water and from groundwater. Samples from tributary streams emerging from snowfields or glaciers, and the Dudh Koshi River which accumulates the flow from these tributaries as well as the Khumbu Glacier, may represent sources with varying scales of recharge areas and thus residence time—glacial melt can arise from ice that has experienced many years of accumulation and ablation. Similarly, groundwater samples also arise from watersheds of various sizes and thus residence times. Hillside seeps with steep slopes and thin soils may reflect melt from recharge accumulated in a single year. Larger springs, that serve as community water sources, discharge groundwater from larger watersheds of talus and glacial moraine which may homogenize the effects of several monsoon cycles and evaporation and are more resilient to short term drought conditions.

In contrast, the data from the Niyang River watershed are more tightly clustered along the LWL. No groundwater samples are included in the dataset from this semi-arid landscape and the sources of water in the tributaries and the Niyang River derive from annual snowmelt at high elevation and monsoonal rainfall at lower elevations (which may both exceed the potential evapotranspiration) rather than the limited geographic scope of glaciers in the watershed. Therefore, the sources of water for the Tibetan Plateau samples are less likely to span multiple years of recharge. It is important to emphasize the similarities between these isotopic values between the data in this study and published datasets. It is also important to note that although two years separate the samples in this study, the regional climate conditions were similar at the time of collection (it is noteworthy that the ONI index indicated stronger La Niña conditions leading up to the collection of the Tibetan Plateau samples).

5.2. Altitude effect

The altitude lapse rate for the Dudh Koshi River watershed ($-2.8‰\ km^{-1}$ for $\delta^{18}O$) is like the Seti River in the central Himalaya ($-2.9‰\ km^{-1}$ for $\delta^{18}O$; Garzione et al., 2000), and the Brahmaputra River ($-2.9‰ \cdot km^{-1}$ for $\delta^{18}O$; Hren et al., 2009); however, the lapse rate for tributaries streams is similar (Fig. 4A) to the Boqu River in southern Himalaya in 2006 ($-3.6‰\ km^{-1}$ for $\delta^{18}O$; Wen et al., 2012). The isotopic composition of river waters is the average of all sources of water from upstream of the sampling site and may thus bias toward significantly higher elevations. Thus, the lapse rate for groundwater samples ($-2.5‰\ km^{-1}$ for $\delta^{18}O$), with smaller recharge areas, may be a more accurate representation of the true lapse rate for precipitation (Darling et al., 2003) as measured elsewhere in the southern and western Himalayas ($-2.3‰\ km^{-1}$ for $\delta^{18}O$; Wen et al., 2012; Jeelani et al., 2013). The similarity between these lapse rate data suggest, but do not conclude, that the clustering of mountain peaks above 8,000 ma.s.l. has limited effect on the lapse rate values in the Dudh Koshi River watershed.

The altitude lapse rate for the Niyang River watershed ($-3.1‰\ km^{-1}$ for $\delta^{18}O$) mimics the results from the Lhasa River on the Tibetan Plateau (Yao et al., 2009). Like the results from Nepal, the lapse rate for the tributary streams ($-4.1‰\ km^{-1}$ for $\delta^{18}O$) is much higher than for the river ($-2.1‰\ km^{-1}$ for $\delta^{18}O$) (Fig. 5); the water in the tributaries derives from significantly higher elevations than the sampling site. Similarly, the measured lapse rate for precipitation ($-1.1‰\ km^{-1}$ for $\delta^{18}O$; Dailai et al., 2002) is significantly lower than for river water samples.

Lapse rates are commonly assessed using linear regressions; however, the data from this study suggest that isotopic values may level-off at higher altitudes (e.g., samples above 4,500 ma.s.l. in Figs. 3-5), possibly due to the formation of snow. On the slopes of Dunagiri in the southern Himalaya near Garhwal, India, no altitude effect was measured at altitudes from 4500 to 6,000 ma.s.l. where Niewodnizcanski et al. (1981) hypothesized that the reduction in the altitude effect may result from precipitation from high clouds mantling the summits, excessive ablation, and the exceptional climates conditions (wind) at high altitude.

6. Conclusion

We present $\delta^{18}O$ and δD, d-excess, LWLs, and altitude lapse rates for river water and groundwater seeps and springs sampled in the Dudh Koshi River watershed in the High Himalayas of eastern Nepal (March 2013) and in the Niyang River watershed in the Eastern Nyainqentanghla Mountains of the Tibetan Plateau (May 2011). Both sets were collected during the non-monsoon season and in periods of negative ONI index. The results are complementary to other regional climate and watershed studies that illustrate that waters in the High Himalayas are more influenced by marine moisture sources (mean d-excess = 7.4‰ ± 4.5‰) and more evaporation at warmer temperatures, $\delta D = (7.8‰ \pm 0.3‰) \cdot \delta^{18}O + (4.0‰ \pm 4.6‰)$, than those on the Tibetan Plateau comprised of recycled continental moisture at cooler temperatures (mean d-excess = 13.1‰ ± 2.0‰; $\delta D = (8.7‰ \pm 0.\ 1‰) \cdot \delta^{18}O + (24.3‰ \pm 2.0‰)$). Decreasing elevation, via increased air temperature, results in higher d-excess values; the dominance of glacial melt on the Dudh Koshi River guides the d-excess of those river water samples. Altitude lapse rates of $\delta^{18}O$ and δD for the Nepal samples ($-2.8‰\ km^{-1}$ and $-24.0‰\ km^{-1}$) are neither significantly different from samples from the Tibetan Plateau ($-3.1‰\ km^{-1}$ and $-27.0‰\ km^{-1}$) nor elsewhere in southern Himalaya; the density of peaks exceeding 8,000 ma.s.l. does not appear to influence the non-monsoon lapse rates. The data from this study also include a trend toward reduced lapse rates at altitudes greater than 4,500 ma.s.l., the product of a reduced altitude effect from extreme climate conditions. These results enhance a comprehensive understanding of the hydrological cycle in the Himalayas.

Acknowledgements

We thank C. Spielbauer and L. Etchison for assisting with the measurement of water samples at the Department of Earth Sciences, IUPUI. K. Nicholson and K. Neumann at Ball State University organized and led the field study in Nepal; sincere gratitude to Mohan and his Sherpa team for safe leadership to Everest Base Camp. IGS colleagues improved the quality of this manuscript prior to external anonymous review. The authors are also grateful for anonymous and editor reviews of an earlier version of this manuscript. This research did not receive any specific grant from funding agencies in the public, commercial, or not-for-profit sectors.

References

Ambach, W., 1968. The altitude effect on the isotopic composition of precipitation and glacier ice in the Alps. Tellus 20, 595–600.
Bershaw, J., Penny, S.M., Garzione, C.N., 2012. Stable isotopes of modern water across the Himalaya and eastern Tibetan Plateau: implications for estimates of paleoelevation and paleoclimate. J. Geophys. Res. 117, D02110. http://dx.doi.org/10.1029/2011JD016132.
Bowen, G.J., Wilkinson, B., 2002. Spatial distribution of d 18O in meteoric precipitation. Geology 30 (4), 315–318.
Clark, I., Fritz, P., 1997. Environmental Isotopes in Hydrogeology. Lewis Publishers, New York, pp. 352.
Craig, H., 1961. Isotopic variation in meteoric waters. Science 133, 1702–1703.
Dailai, T.K., Bhattacharya, S.K., Krishnaswami, S., 2002. Stable isotopes in the source waters of the Yamuna and its tributaries: seasonal and altitudinal variations and relation to major cations. Hydrol. Process. 16, 3345–3364.
Dansgaard, W., 1964. Stable isotopes in precipitation. Tellus 16, 436–468.
Darling, W.G., Bath, A.H., Talbot, J.C., 2003. The O & H stable isotopic composition of fresh waters in the British Isles. 2. Surface waters and groundwater. Hydro. Earth Syst. Sci. 7 (2), 183–195.
Fan, Y., Chen, Y., Li, X., Li, W., Li, Q., 2014. Characteristics of water isotopes and ice -snowmelt quantification in the Tizinafu River, north Kunlun Mountains, Central Asia. Quat. Int. 380–381. http://dx.doi.org/10.1016/j.quaint.2014.05.02.
Feng, F., Feng, Q., Liu, X., Wu, J., Liu, W., 2017. Stable isotopes in precipitation and atmospheric moisture of pailugou catchment in northwestern China's Qilian Mountains. Chin. Geogr. Sci. 27 (1), 97–109. http://dx.doi.org/10.1007/s11769-017-0849-y.
Garzione, C.N., Quade, J., DeCelles, P.G., English, N.B., 2000. Predicting paleoelevation of Tiben and the himalaya from $\delta^{18}O$ vs altitude gradients in meteoric water across the Nepal Himalaya. Earth Planet Sci. Lett. 183, 215–229.
Gat, J.R., Matsui, E., 1991. Atmospheric water balance in the Amazon Basin: an isotopic evapo-transpiration model. J. Geophys. Res. 96, 179–188.
Gat, J.R., 1996. Oxygen and hydrogen isotopes in the hydrologic cycle. Annu. Rev. Earth Planet Sci. 24, 225–262.
Geldern, R., Barth, J.A., 2012. Optimization of instrument setup and post-run corrections for oxygen and hydrogen stable isotope measurements of water by isotope ratio infrared spectroscopy (IRIS). Limnol. Oceanogr. Methods 10, 1024–1036.
Hren, M., Bookhagen, B., Blisniuk, P., Booth, A., Chamberlain, C., 2009. $\delta^{18}O$ and dD of streamwaters across the Himalaya and Tibetan Plateau: implications for moisture sources and paleoelevation reconstructions. Earth Planet Sci. Lett. 288, 20–32. http://dx.doi.org/10.1016/j.epsl.2009.08.041.
IVPA, 2011. World Maps of Köppen-Geiger Climate Classification, Institutes for Veterinary Public Health. (viewed from). http://www.koeppen-geiger.vu-wien.nc.at/shifts.htm.
Jeelani, G., Saravana Kumar, U., Kumar, B., 2013. Variation of δ^{18} O and δD in precipitation and stream waters across the Kahir Himalaya (India) to distinguish and estimate the seasonal sources of stream flow. J. Hydrol. 481, 157–165.
Liu, Z., Tian, L., Yao, T., Yu, W., 2008. Seasonal deuterium excess in nagqu precipitation: influence of moisture transport and recycling in the middle of Tibetan Plateau. Environ. Geol. 55 (7), 1501–1506.

Manfredi, E.C., Flury, B., Viviano, G., Thakuri, S., Khanal, S.N., Jha, P.K., Maskey, R.K., Kayastha, R.B., Kafle, K.R., Bhochhobhoya, S., Ghimire, N.P., Shrestha, B.B., Chaudhary, G., Giannino, F., Carteni, F., Mazzoleni, S., Salerno, F., 2010. Solid waste and water quality management models for sagarmatha national park and buffer zone, Nepal : implementation of a participatory modeling framework. Mtn. Res. Dev. 30 (2), 127–142.

NOAA, 2017. Cold and Warm Episodes by Season, National Weather Service Climate Prediction Center, National Oceanic and Atmospheric Administration. (viewed from). http://www.cpc.ncep.noaa.gov/products/analysis_monitoring/ensostuff/ensoyears.shtml, accessed 2/14/2017.

Niewodnizcanski, J., Grabczak, J., Barański, L., Rzepka, J., 1981. The altitude effect on the isotopic composition of snow in high mountains. J. Glaciol. 27, 99–111.

Olson, D.M., Dinerstein, E., Wikramannayake, E.D., Burgess, N.D., Powell, G.V.N., Underwood, E.C., D'Amico, J.A., Itoua, I., Strand, H.E., Morrison, J.C., Loucks, C.J., Allnutt, T.F., Ricketts, T.H., Kura, Y., Lamoreux, J.F., Wettengle, W.W., Hedao, P., Kassem, K.R., 2001. Terrestrial ecoregions of the world: a new map of life on Earth. Bioscience 51, 933–938.

Pande, K., Padia, J.T., Ramesh, R., Sharma, K.K., 2000. Stable isotope systematics of surface water bodies in the himalayan and trans-himalayan (Kashmir) region. Proc. Indian Acad. Sci. 190, 109–115.

Pang, H.X., He, Y.Q., Zhang, Z.L., Lu, A., Gu, J., 2004. The origin of summer monsoon rainfall at New Delhi by deuterium excess. Hydrol. Earth Syst. Sci. 8 (1), 115–118. http://dx.doi.org/10.5194/hess-8-115-2004.

Peel, M.C., Finlayson, B.L., McMahon, T.A., 2007. Updated world map of the Köppen-Gaiger climate classification. Hydrol. Earth Syst. Sci. 11, 1633–1644.

Tian, L., Masson-Delmotte, V., Stievenard, M., Yao, T., Jouzel, J., 2001. Tibetan Plateau summer monsoon northward extent revealed by measurements of water stable isotopes. J. Geophys. Res. 106 (D22). http://dx.doi.org/10.1029/2001JD900186. (28, 081-28, 088).

Wang, L., Caylor, K., Dragoni, D., 2009. On the calibration of continuous, high-precision $\delta^{18}O$ and $\delta^{2}H$ measurements using an off-axis integrated cavity output spectrometer. Rapid Commun. Mass Spectrom. 23, 530–536.

Wang, L., Caylor, K.K., Villegas, J.C., Barron-Gafford, G.A., Breshears, D.D., Huxman, T.E., 2010. Partitioning evaportranspiration across gradients of woody plant cover: assessment of a stable isotope technique. Geophys. Res. Lett. 37, L09401. http://dx.doi.org/10.1029/2010GL043228.

Wen, R., Tian, L.D., Weng, Y.B., Liu, Z.F., Zhao, Z.P., 2012. The altitude effect of $\delta^{18}O$ in precipitation and river water in the Southern Himalayas. Chin. Sci. Bull. 57, 1693–1698.

Yao, T.D., Zhou, H., Yang, X.X., 2009. Indian monsoon influences altitude effect of $\delta^{18}O$ in precipitation/river water on the Tibentan Plateau. Chin. Sci. Bull. 54, 2724–2731.